Predicting duststorm evolution with the vorticity theory

H. Choi [a,b,*], Y.H. Zhang [b]

[a] *Department of Atmospheric Environmental Sciences, Kangnung National University, Kangnung, Kangwondo 210-702, Republic of Korea*
[b] *State Joint Key Lab of Environmental Simulation and Pollution Control, College of Environmental Sciences, Peking University, Beijing 100871, China*

A B S T R A C T

The relationship between duststorms and vorticity in Mongolia and northern China was investigated from March 19–31, 2001, using the three-dimensional, nonhydrostatic, mesoscale model (MM5). At the 500-hPa level, the area of maximum negative relative vorticity, or strong upward motion of air, coincided with the area of duststorm generation in Neimongo of northwestern China when relative humidity was less than 40% and wind speed was greater than 10 m s^{-1}. The transport of dust arising from the source region always followed the negative vorticity area downwind. This region of duststorm generation was the same as the layer of unstable atmospheric air (negative potential vorticity layer) near the ground surface in the vertical distribution of baroclinic potential vorticity, which was a function of diabatic heating and frictional terms with respect to time.

During the day, dust parcels were lifted to about 700 hPa (about 3 km) where the potential temperature gradient with pressure ($\partial\theta/\partial p$) was zero. The height of these dust parcels was confined to the 700-hPa level where stability extended to the stratosphere. The convective boundary layer (negative potential vorticity value) extended to about 1 km, and initially dust particles floated from the ground surface to the mixed layer of about 1.5 km above the convective boundary layer where they remained. The westerly wind drove the particles downwind. At night, a shallow stable boundary layer near the ground surface (inversion layer, large positive potential vorticity) developed, and the particles inside the stable layer merged near the ground and moved downwind. The dust particles in the mixed layer still moved downwind, and dry deposition occurred from the top of the stable layer to the ground surface.

© 2008 Published by Elsevier B.V.

1. Introduction

Duststorms, alternatively called sandstorms, Yellow Sand, or KOSA (Asian dust), represent a severe meteorological phenomenon where strong winds blow a great amount of sand and dust (even small rock) from deserts or arid areas into the lower troposphere. These particles travel long distances reaching several thousand kilometers and can result in the reduction of visibility to less than 1 km. As air turbidity increases with the occurrence of duststorms, the amount of solar radiation reaching the ground surface is reduced, which can exert a large influence on the Asian climate and even influence the climate of the North Pacific Ocean as far as North America.

Asian dust mainly originates from elevated ground surfaces at 1500 m above sea level in the Taklamakan, Gobi, and Ordos deserts and the Loess plateau and generally occurs seasonally when the spring is dry. The threshold value of wind speed for dust mobilization in the Loess Plateau and Gobi desert ranges from 10–12 m s^{-1} from field observations and wind tunnel experiments (Jigjidsuren and Oyuntsetseg, 1998; Middleton, 1986; Natsagdorj and Jugder, 1992a,b; Jungder, 1999; Qian and Hu, 1997; Wang et al., 2003). Xuan and Sokolik (2002) suggested that the threshold value of friction velocity ranged from 25–70 cm s^{-1}, depending on particle size and soil

type. Tegen and Fung (1994) and Zhang and Zhong (1985) concluded that regions where duststorms occur for more than 30 days per year coincide with regions where relative humidity (RH) is less than 40%, which represents the surface water content in the soil layer.

To estimate the quantity of dust transported from the origin, statistical methods have been used, and numerical simulations have been performed. Unfortunately, most of these research results have not produced an adequate explanation for the generation of duststorms from a meteorological perspective, even though synoptic-scale, meteorological explanations, using mainly weather charts and other meteorological fields highlighting strong wind fields near the ground surface, are possible. The meteorological approach usually focuses on duststorm generation and associated weather by analyzing the synoptic weather situation (Austin and Midgley, 1994; Carmichael et al., 1997; Chen et al., 1991; Chon, 1994; Chung and Yoon, 1996; Chung et al., 2003; Reed, 1979; Reed and Albright, 1986). To quantitatively estimate the duststorm, most studies have focused on evaluating the quantity of dust lifted into the atmosphere, but unfortunately there has not been much explanation regarding the generation of duststorms from meteorological perspectives, such as atmospheric boundary layer processes and atmospheric circulation, which could induce the formation of duststorms (Choi et al., 2004).

Thus, the objective of this study was to develop a technique for predicting the formation of duststorms and to use the vorticity theory to explain how the generation mechanisms affect the formation of duststorms, as well as the propagation area for the storms. This study focuses on the contribution of baroclinic potential vorticity (PV) to the development of the atmospheric boundary layer and vertical and horizontal dispersion of dust in the vicinity of source regions.

2. Numerical method and vorticity theory

2.1. Numerical model and input data

A three-dimensional, nonhydrostatic version of MM5 (v3.5) employing an isentropic vertical coordinate was used to investigate meteorological conditions associated with the generation of duststorms during March 18–25, 2001. Three-dimensional NCEP (National Weather Service, National Centers for Environmental Prediction) data with a horizontal resolution of 2.5°×2.5°, including topography, vegetation, snow cover or water, meteorological elements of wind velocity, temperature, moisture content, heat budget, sea surface temperature, and sounding data from the ground surface to 100 hPa, were used as initial conditions for the coarse-mesh domain. Then, interpolated input data were triply nested first at 27 km (125×105 grid points) with 23 vertical levels, then at 9 km (82×82 grid points), and finally at 3 km (61×61 grid points). The 2.5° resolution terrain data were used for the coarse-mesh domain, and then 0.9-km resolution terrain data were used for the fine-mesh domain.

The MRF (medium-range forecast) (or Hong–Pan) scheme (Hong and Pan, 1996) for cumulus parameterization was adopted in the planetary boundary layer, and a simple ice scheme with no supercooled water and immediate melting of snow below freezing level was also used. After the nesting process from large to small domains, a west–east cross-section along the path of the dust was made from the point of generation in western China to Japan in order to investigate the vertical structure of wind, temperature, RH, total cloud-mixing ratio, and vertical velocity. In the large domain, a line was drawn through Neimongo, Beijing, Seoul, Kyoto, and the Pacific Ocean from the latitude/longitude coordinates of (10, 90) to (130, 40) (Fig. 1).
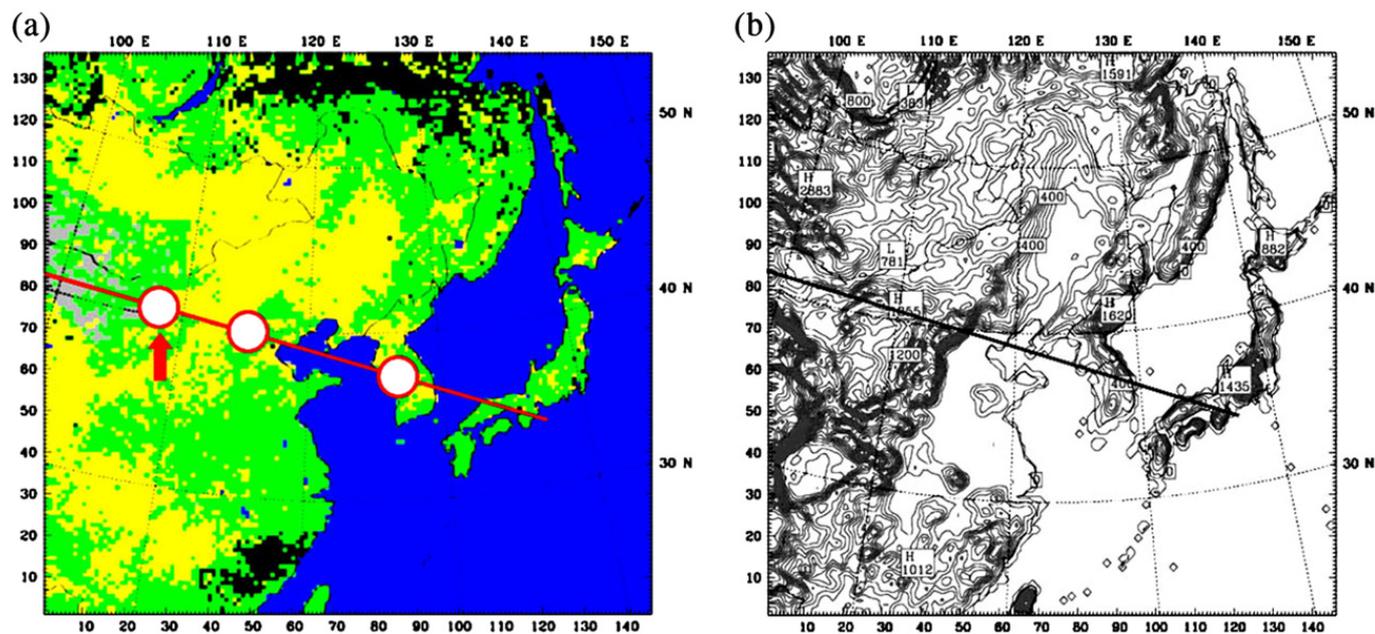
Fig. 1. (a) Land-use data and (b) topography for the coarse-mesh domain—horizontal grid size of 27 km for MM5 model. In (a), circles on straight red line denote Neimongo (left; thick arrow) where duststorms were usually generated—Beijing (center) in China and Seoul (right) in Korea.

(a)

(b)
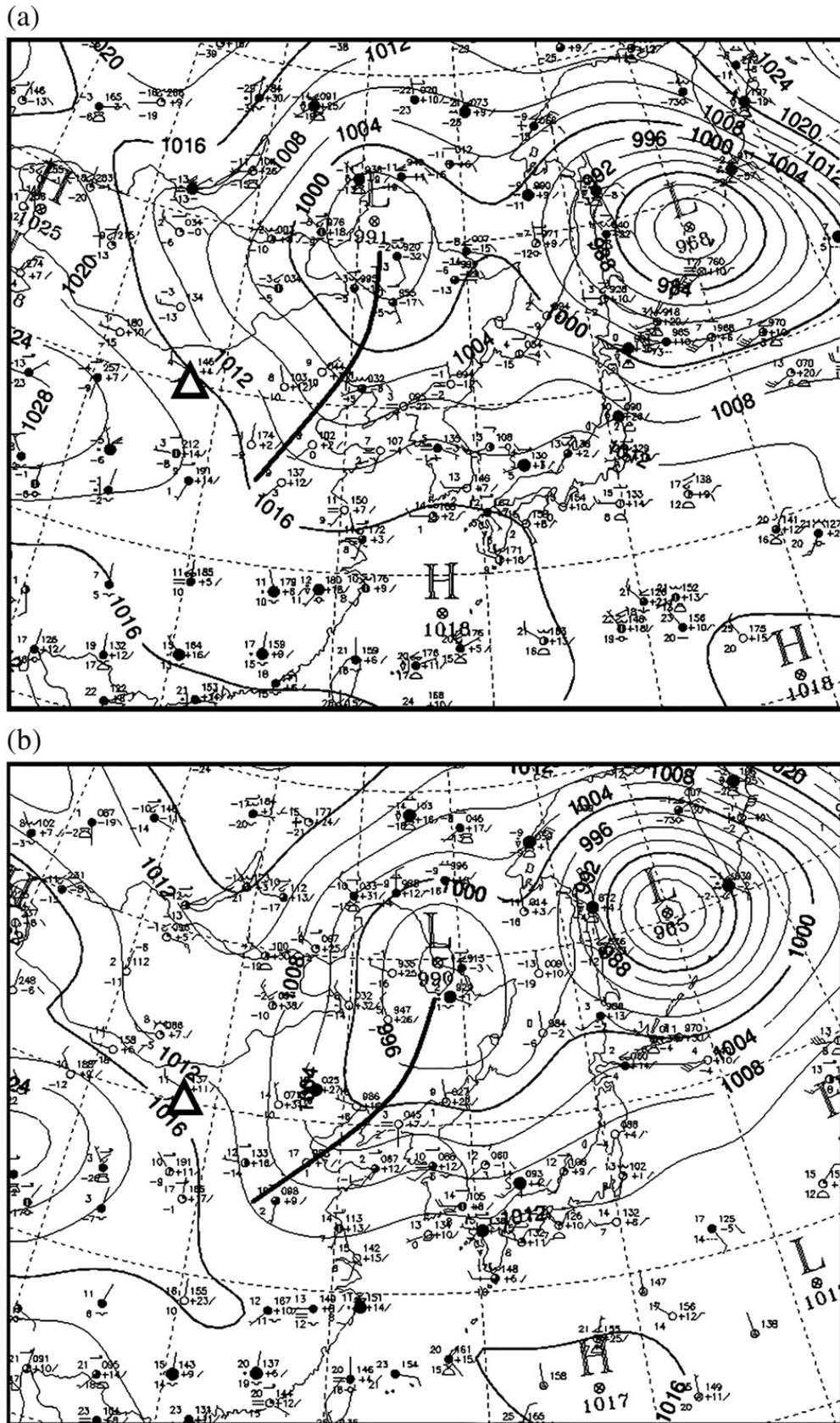
Fig. 2. Surface weather chart at (a) 0000 UTC (0900 LST) and (b) 1200 UTC, March 19, 2001. Triangle and thick-curved line in (a) denote Neimongo area with frequent occurrence of duststorms and cold front.
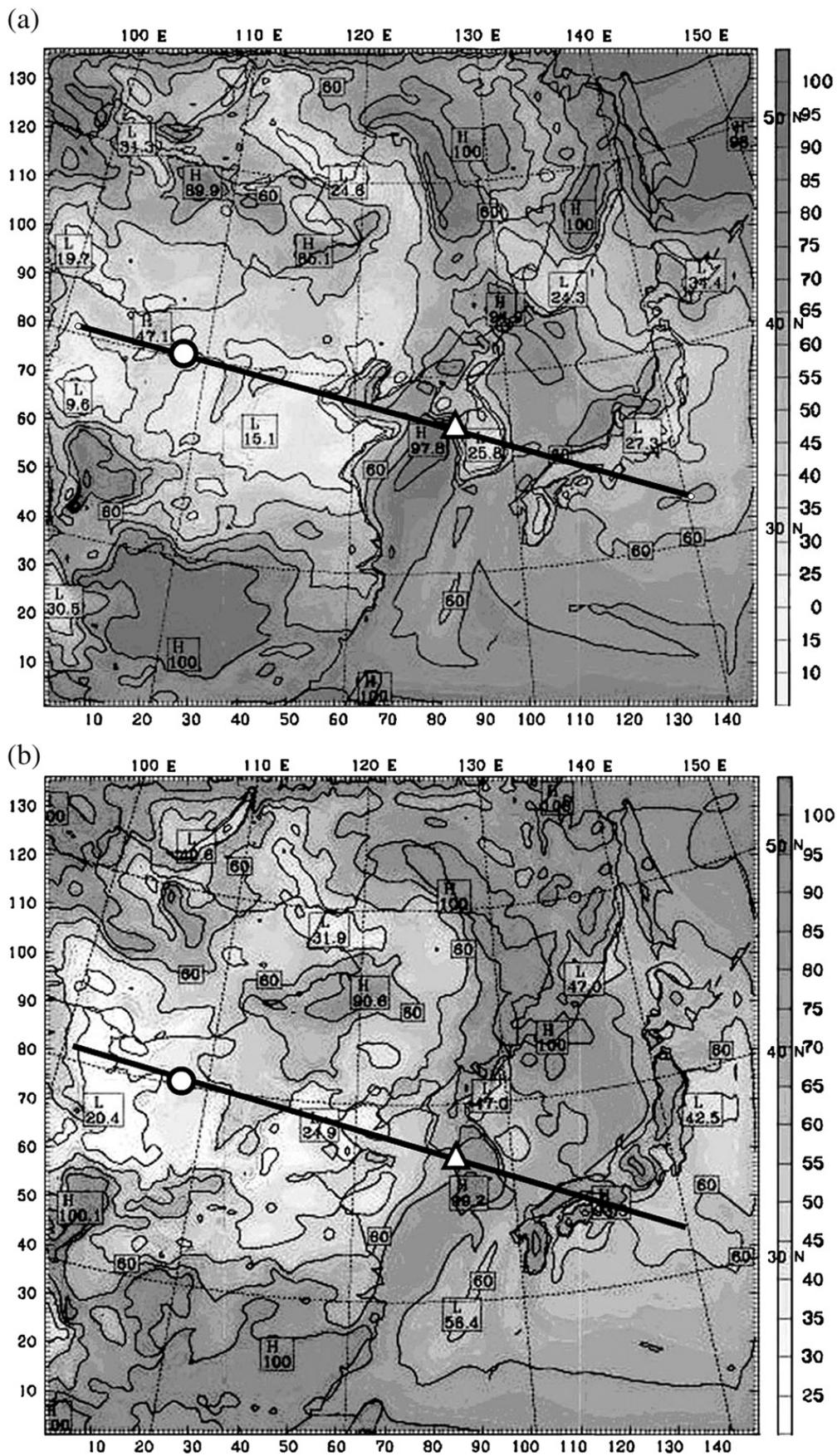
Fig. 3. Relative humidity (RH; %) at 10 m height at (a) 0000 UTC and (b) 1200 UTC, March 19, 2001, from MM5 model simulations. Interval of RH contour is 15%. A straight line from the NW to the SE passing through Neimongo area (circle; RH 35–45%), Beijing (China), Seoul (triangle; Korea), and Kyoto (Japan).
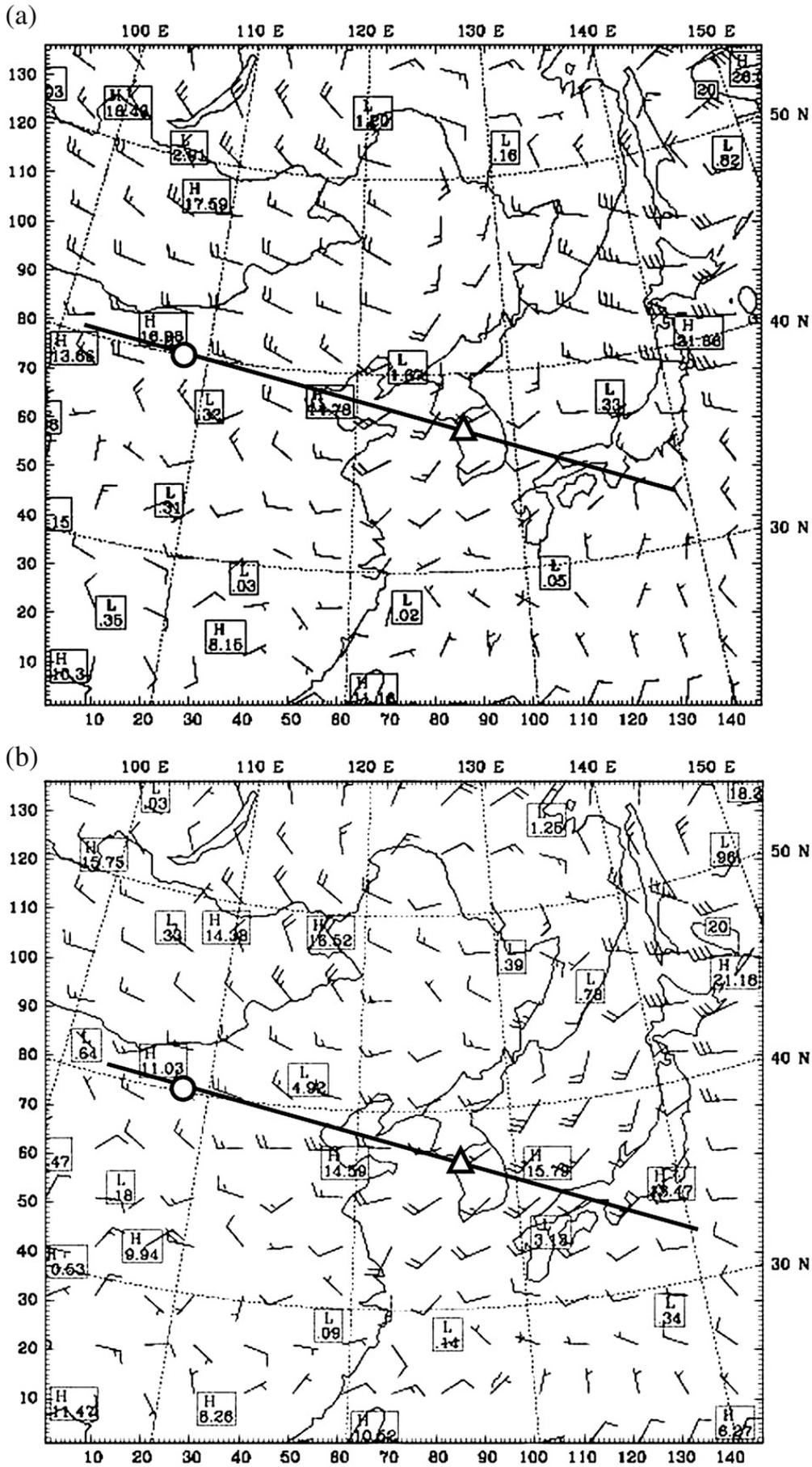
Fig. 4. Wind speed (m s^{-1}) at (a) 0000 UTC and (b) 1200 UTC, March 19, 2001, from MM5 model simulations. Full barb is 5 m s^{-1}. Circle and triangle denotes Neimongo area (wind speed over than 10 m s^{-1}) and Seoul, Korea.
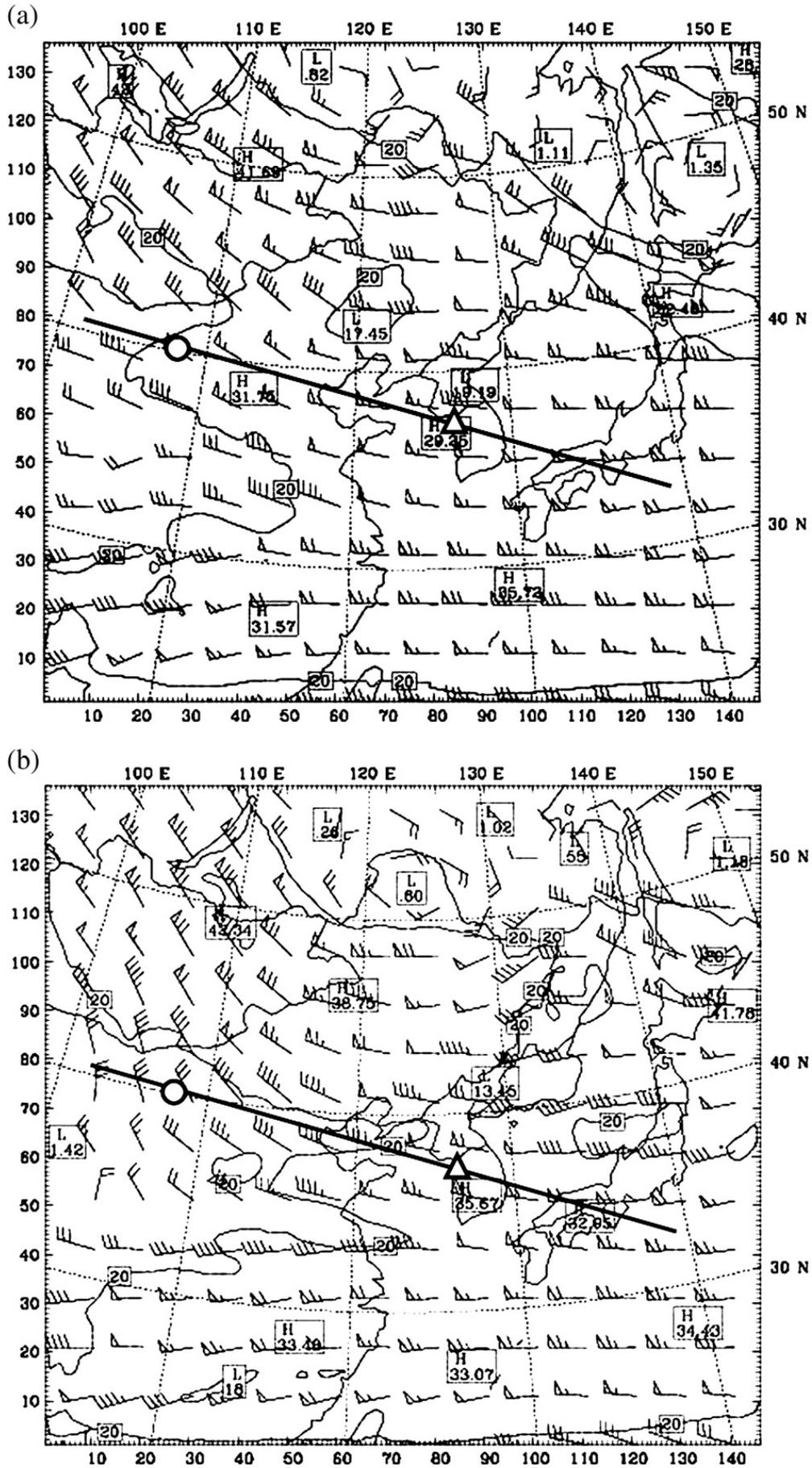
Fig. 5. Wind speed (m s^{-1}) at 500 hPa level at (a) 0000 UTC and (b) 1200 UTC, March 19, 2001, from MM5 model simulations. Full barb is 5 m s^{-1}.

2.2. Vorticity theory

Rossby (1937, 1940) found that PV on isentropic surfaces was conserved for frictionless and adiabatic flow. Potential vorticity is generally defined by the variation of potential temperature to atmospheric pressure with height. Reed and Sanders (1953) used PV as a tracer and explained that air in middle- and upper-tropospheric fronts originate in the stratosphere. Chen et al. (1991), Reed (1979), Reed and Albright (1986), and Sanders and Gyakum (1980) explained cyclogenesis and the development of a frontal zone using the vorticity theory in detail. Later, on the figures produced from results of the numerical simulation on PV using the MM5 model in this study, a large value for PV was shown in the upper-tropospheric atmosphere and sometimes was folded into the lower atmosphere. Haynes and McIntrye (1987) showed that PV could be diluted or concentrated only by flow across isentropes, and PV cannot be created or destroyed within a layer bounded by isentropic surfaces.

However, if diabatic heating or frictional torques are present, PV is no longer conserved. This means that PV can be created or destroyed and drawn away from the isentropes. Therefore, if we consider the frictional term with the diabatic vertical and horizontal advection terms of the horizontal momentum equation in isentropic coordinates, the total derived isentropic PV equation is given by

$$\frac{\tilde{D}P}{Dt} = \frac{\partial P}{\partial t} + \vec{V} \cdot \nabla_\theta P = \frac{P}{\sigma}\frac{\partial}{\partial \theta}(\sigma\dot{\theta}) + \sigma^{-1}k \cdot \nabla_\theta \times \left(\dot{F}_r - \dot{\theta}\frac{\partial V}{\partial \theta}\right) \quad (1)$$

Here the density in (x, y, θ) space is defined as $\sigma \equiv -g^{-1}\partial P/\partial\theta$, and $P \equiv (\zeta_\theta + f)/\sigma$ is Ertel PV, considering the diabatic term as the first on the right-hand side and frictional term as the second. If the diabatic and frictional terms can be evaluated, it is possible to determine the evolution of P following the horizontal motion on an isentropic surface. When the diabatic and frictional terms are small, PV is approximately conserved following the motion on isentropic surfaces. However, weather disturbances that have sharp gradients in dynamic fields, such as jets and fronts and even the generation of duststorms, are associated with large anomalies in the Ertel PV (baroclinic PV) within the nonhydrostatic atmosphere (Holton, 1992; Bluestein, 1993).

At 500 hPa and 1000 hPa (near the ground surface), there is a strong vertical motion on the right-hand side of the trough of geopotential height at 500 hPa above the warm sector on the right-hand side of the cold front at the ground surface, owing to differential relative vorticity advection and temperature advection. The Ertel PV theory usually focuses on relatively large-scale motion of air with regard to small-scale disturbances of less than a few thousand kilometers, but this theory is adapted to the atmospheric boundary layer and comparatively much smaller-scale phenomena than synoptic-scale disturbances. In these cases, the value of a PV unit (PVU) does not need to be positive but can be negative or positive in the atmospheric boundary layer.

3. Result and discussion

3.1. Vorticity effect on generation of duststorms

At the beginning of the duststorm occurring at 0000 UTC (0800 in China; 0900 LST in Korea) on March 19, 2001, in Neimongo, RH presenting the moisture content of air adjacent to the soil layer was greater than 40%. With a ground surface wind speed greater than 6 m s^{-1}, dust could not be lifted from
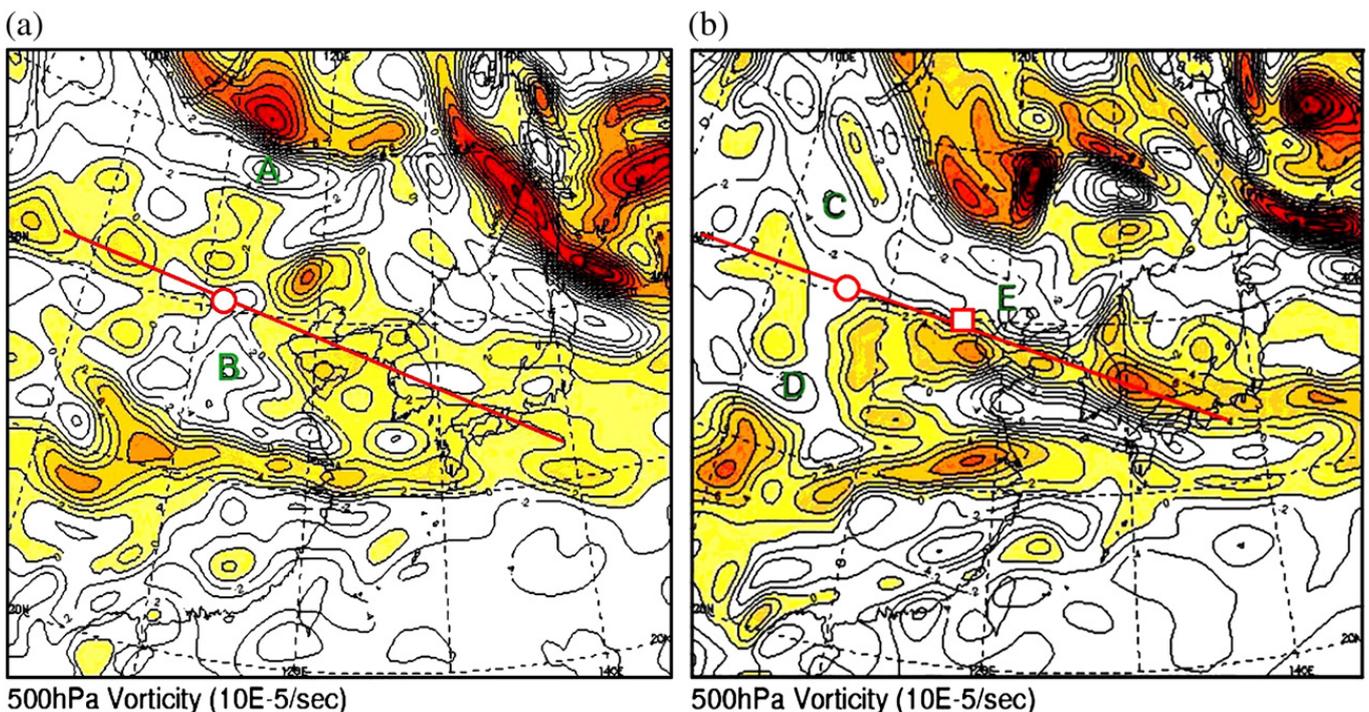
Fig. 6. Relative vorticity (interval of 2×10^{-5} s^{-1}) at the 500-hPa level at (a) 0000 UTC and (b) 1200 UTC, March 19, 2001, was calculated by the MM5 model. White areas (A and B) and both yellow- and red areas denote negative and positive vorticity areas, respectively. Red circle on red straight line above B indicates the generation area of duststorm. The duststorm area in (b) was further extended as shown in Fig. 7, following northwesterly wind in Figs. 4 and 5, and the dust was transported further to the northwest (C), south (D), and east (E) areas near Beijing (red box) of China.

(a) (b)
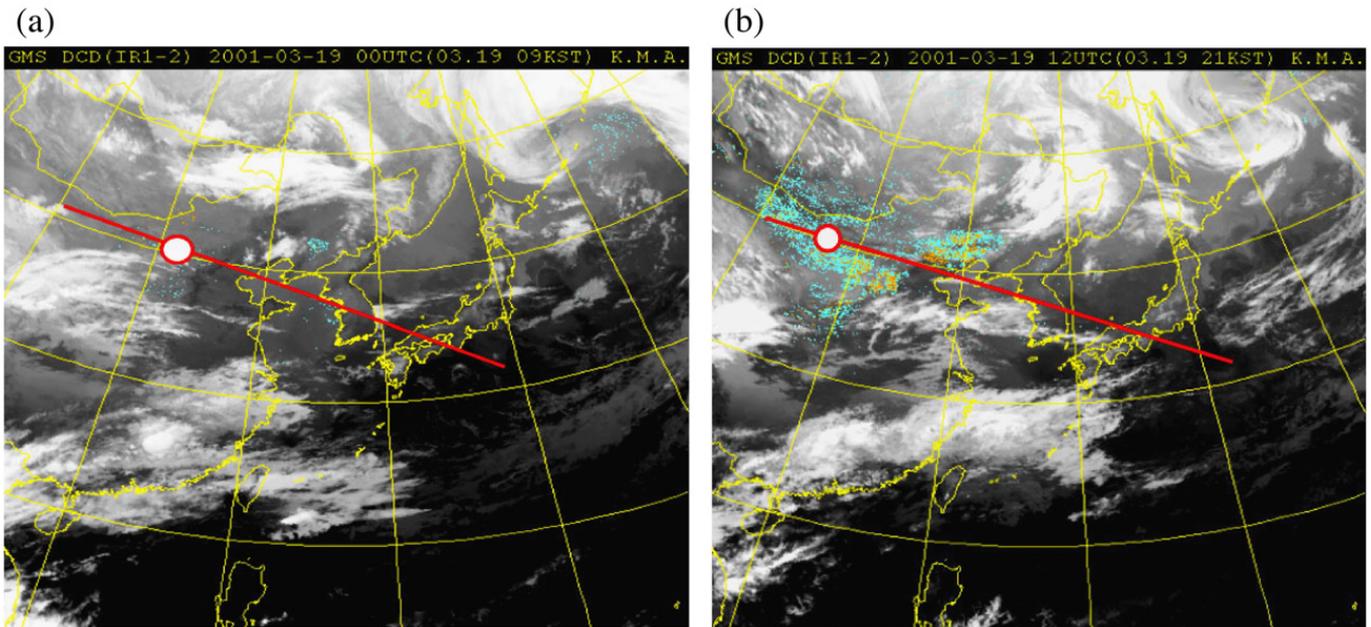
Fig. 7. GMS (DCD-IRI-2) satellite images at (a) 0300 and (b) 1200 UTC on March 19, 2001. Even though at 0000 UTC the GMS satellite image was obscured with clouds, it is possible to detect the dust area by comparing the GMS image with the 1200 UTC image. Duststorm area in (b) coincides with negative vorticity area of C, D, and E in Fig. 6b.

the surface without RH less than 30% (Yamamoto et al., 2003). As Zhang and Zhong (1985) indicate, regions that experience duststorms for more than 30 days also experience a RH of less than 40%. In Neimongo, the RH was approximately 30%, as shown on the weather chart and in the horizontal distribution of RH simulated by MM5 (Figs. 2–4).

A narrow zone of isobaric contours existed from the southern part of Mongolia (northwest) and Neimongo to Zheongzhou (southeast) in China that produced strong northwesterly surface winds greater than 10 m s^{-1} thus making it a

favorable duststorm generation area (Chung et al., 2003). Near the Korean peninsula, the wind direction changed to southwesterly, and dust was transported in the wind direction. At the 500-hPa level, wind was nothwesterly in China and westerly in Korea (Fig. 5). However, at 500 hPa, positive relative vorticity advection was at a maximum above the surface low, while the negative relative vorticity advection was strongest above the high surface.

Fig. 6 shows the relative vorticity area at 500-hPa level. Through a comparison of the vorticity field with a GMS (DCD-

(a) (b)
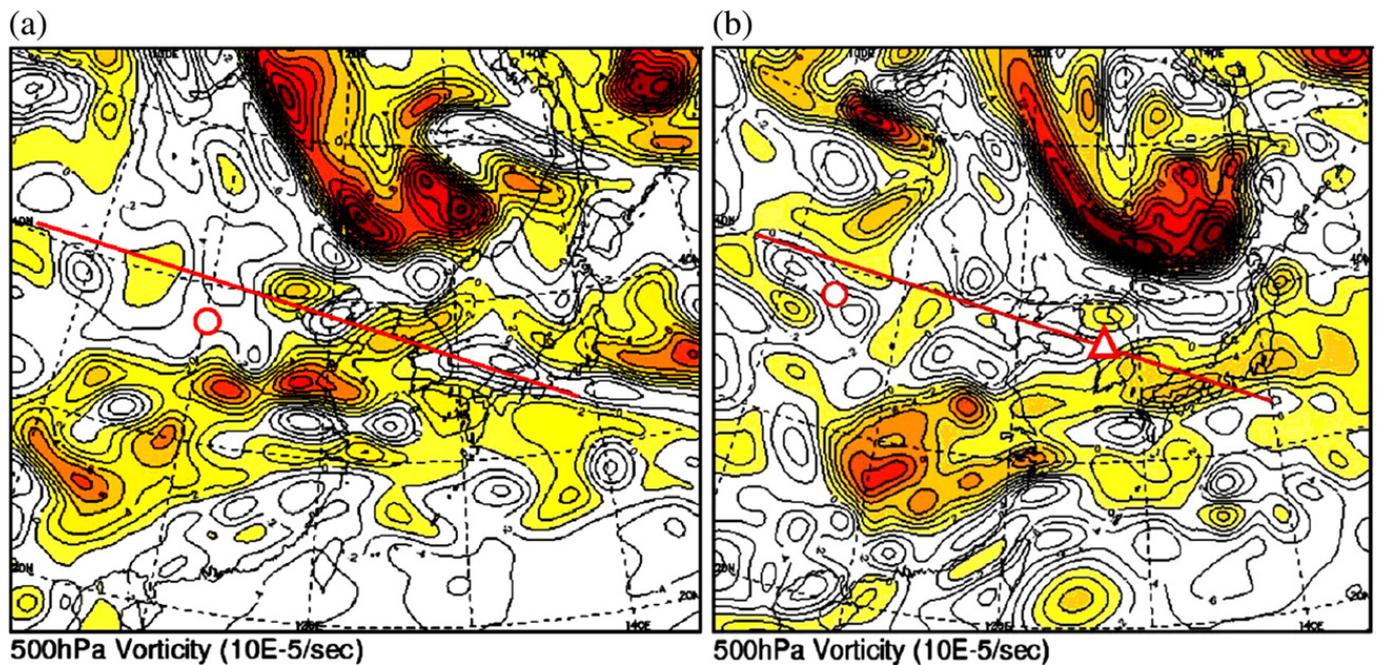
Fig. 8. Vorticity at 500 hPa at (a) 0000 UTC and (b) 1200 UTC on March 20, 2001. Red circle indicates dust area. Red circle and red triangle in (b) denote Gansu province, China, and Seoul, Korea.

(a)

(b)
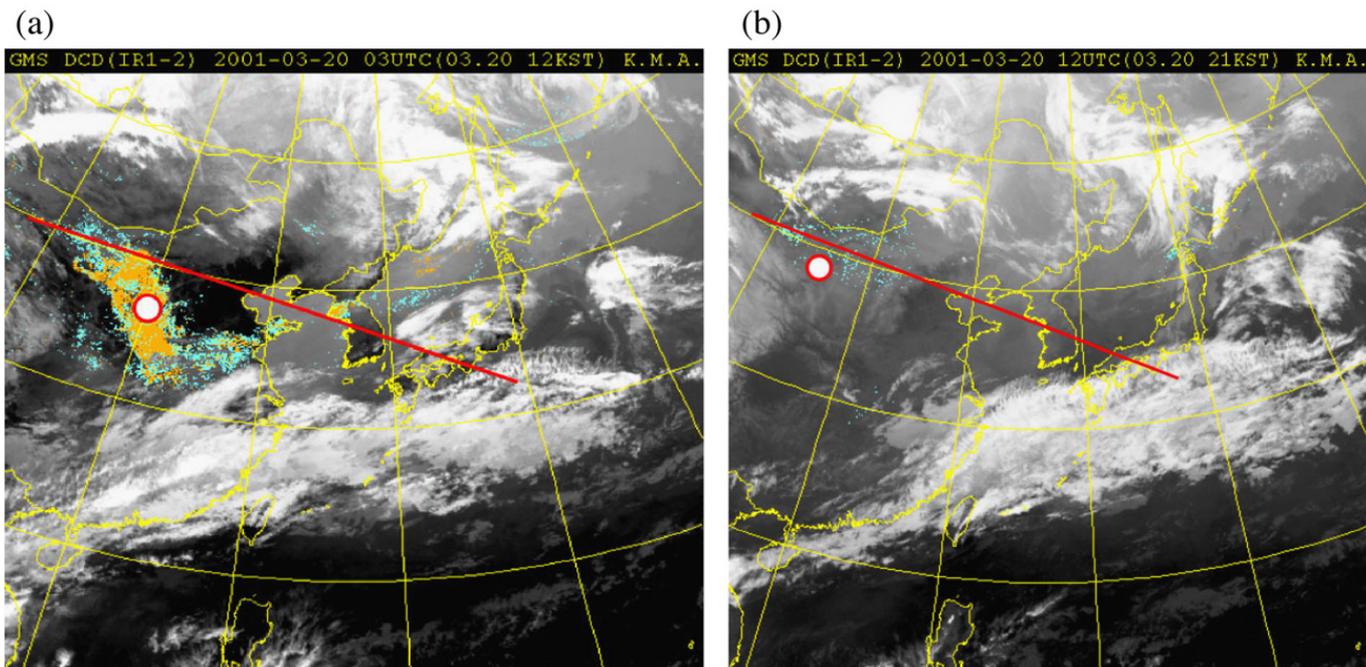
Fig. 9. GMS (DCD-IRI-2) satellite image at 0300 UTC and 1200 UTC on March 20, 2001. Since the image at 0000 UTC was contaminated, the 0300 UTC image is presented. Dust is transported from the duststorm area (red circle) toward the southeastern area (white area) in Fig. 8b and turns toward the northeastern area near the triangle, as shown in Fig. 10b.

IRI-2) satellite image, provided by the Japan Meteorological Agency (Fig. 7) depicting a trace of dust particles, the area of negative, vorticity-inducing upward motion of air, A and B (white), at 0000 UTC on March 19, 2001, directly coincided with the duststorm generation area (not clear due to cloud cover). The transportation area of the dust followed the negative vorticity area stretching westward to Xinjiang province and Mongolia (C), southward to Gansu province (D), and eastward to Manchuria (E) in northeastern China (Fig. 6).

As time passed, the duststorm generation area slightly changed on March 20, 2001, but its maximum, negative relative vorticity area coincided with the duststorm generation area. The dust transport area always followed the negative vorticity area at the 500-hPa level (Figs. 8–10). Because the dust transport area at 1200 UTC March 20, 2001, (Fig. 9b) cannot be seen clearly owing to cloud cover, a GMS-5/VISSR image is additionally given. As shown in Figs. 8–10, dust was transported from the duststorm area (red circle—negative

(a)

(b)
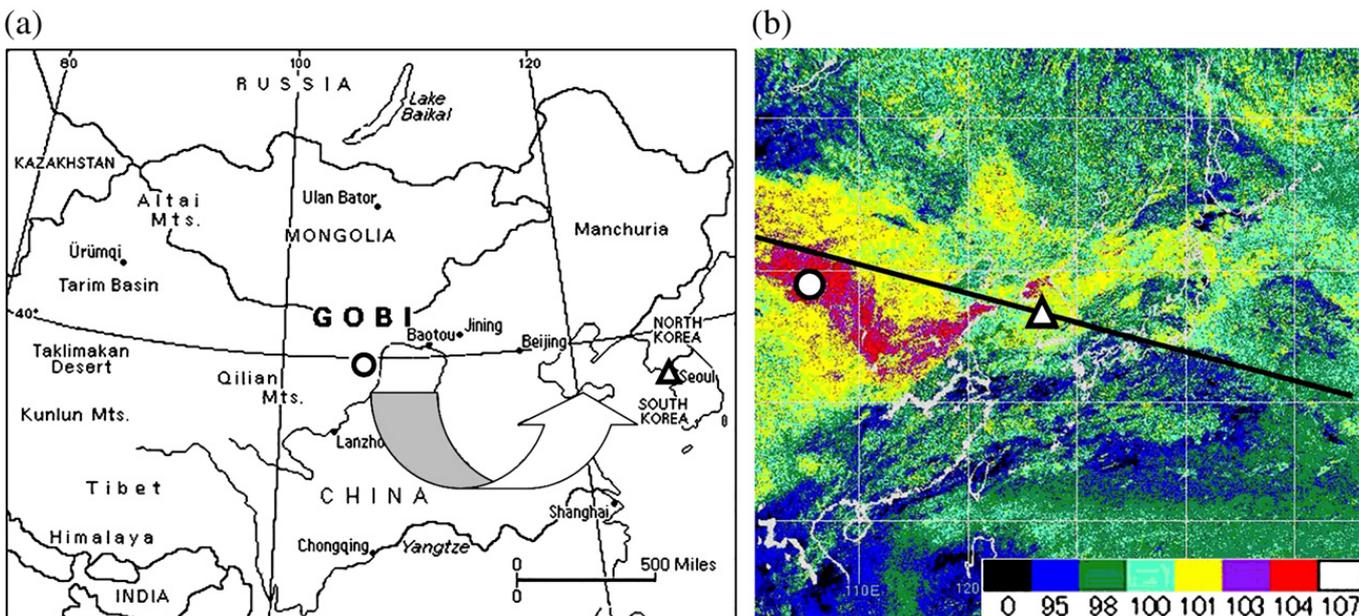
Fig. 10. (a) Map of China and Korea with dust transport route. (b) GMS-5/VISSR image at 1200 UTC on March 20, 2001. Since the satellite image of Fig. 9b was poor owing to cloud cover, additional image is given to compare negative vorticity area at the 500 hPa level in Fig. 8b to the dust generation and transport area. Circle and triangle indicate Neimongo (China) and Seoul (Korea), respectively.
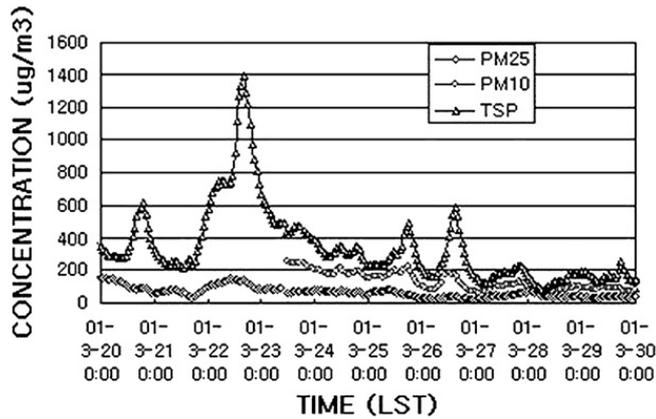
Fig. 11. Hourly based concentrations of $PM_{2.5}$, PM_{10}, and total suspended particulate (TSP) from March 20–30, 2001, when the Seoul district was under duststorm from March 20–25 and non-duststorm periods.

vorticity area) to the southeastern area (white area—negative vorticity area) and turned to the northeastern area near the triangle (Seoul—negative vorticity area) thus showing the dust transport route. It is evident that the Seoul district was subjected to great amounts of dust transported from China.

Under this period, the influence of dust transport toward the Seoul district was verified by ground surface measurement data of dust concentration (Fig. 11). In general, the concentration of total suspended particulate (TSP) in Seoul was confined to less than $100\,\mu g\,m^{-3}$, but under the influence of dust transport from China to the Korean peninsula, the TSP concentration exceeded the $100\,\mu g\,m^{-3}$. The period of the present study was within the period of the Asian Dust event in 2001, which had an un-expectedly high frequency of 27 days from January to May. Measurements were taken only during the March 19–31 period. This period included 13 duststorm and non-duststorm days.

Hourly concentrations for TSP, PM_{10}, and $PM_{2.5}$ were taken near the ground surface and revealed important information regarding the varying concentrations of coarse (TSP) versus fine particles (PM_{10} and $PM_{2.5}$) that occurred between dust-storm and non-duststorm periods. According to the Korean Meteorological Administration report, duststorms were detected from March 20–25 in the Seoul district of Korea, even though the duststorm was generated two days earlier in China. Thus, one can expect that duststorms are generated under RH of less than 40% and wind speed over $10\,m\,s^{-1}$ in the negative vorticity area, and these factors will predict dust transport areas.

At 0000 UTC (0900 LST), March 19, 2001, on the high plain near southern Mongolia and Neimongo in northwest China (Fig. 12a, red circle), a layer of negative PV of less than zero (Fig. 12b) was found over the highest mountain region at a horizontal distance of about 900 km away from the western boundary of the modeling domain. This negative PV of less than zero (white layer) indicated an unstable layer (con-vective boundary layer [CBL]) of about 200 m in depth with a mixed layer (ML) of approximately 1 km deep above the CBL. A positive PV layer with a magnitude greater than 1.5 PVU (black layer) was also found in the surface boundary layer and in the upper troposphere near 400 hPa.

In the upper troposphere, positive PV indicated air coming from the stratosphere into the middle troposphere. Our main concern was confined to the atmospheric boundary layer for dust generation. A positive PV layer near the ground surface, which indicated a stable boundary layer during the day or a nocturnal surface inversion layer at night, reached about 400 m in depth in Neimongo on the upwind side and about 500 m on the downwind side (Fig. 12a,b). At 0300 UTC (1200 LST), the red arrow in Fig. 13b indicated that the height of $\partial\theta/\partial p=0$ and upward motion of air should be limited. A shallow unstable
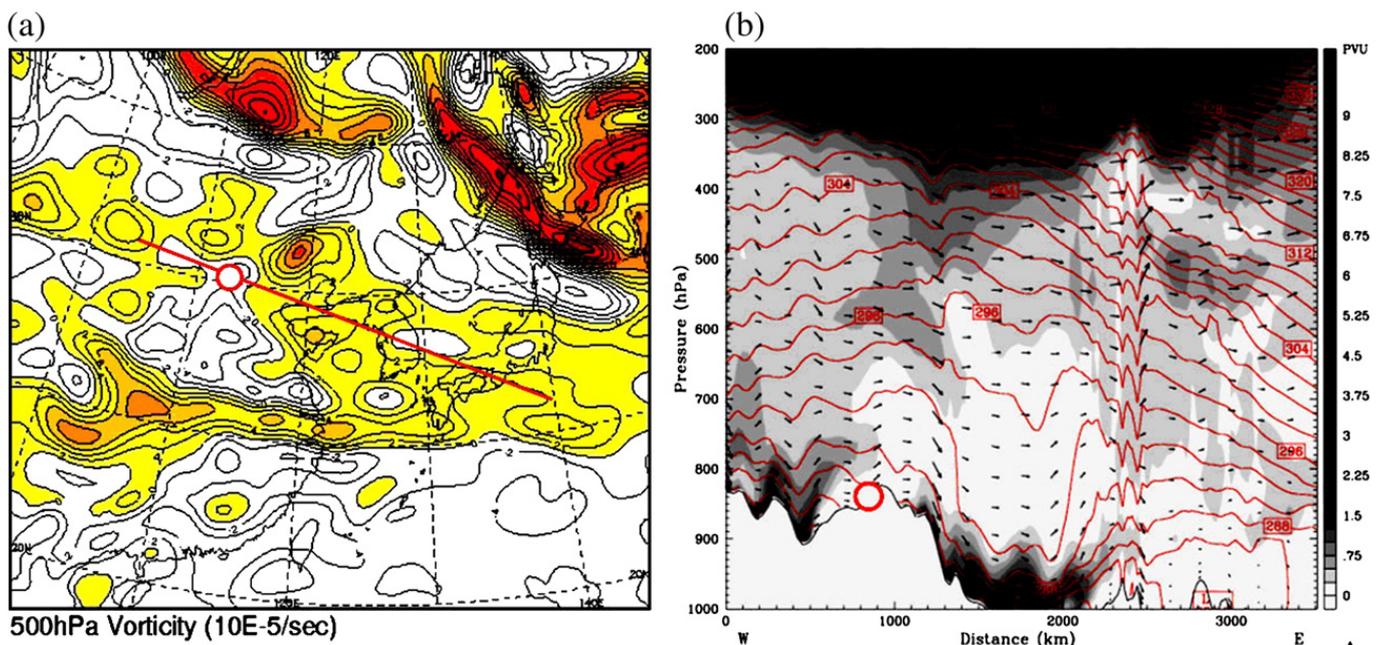
Fig. 12. (a) Relative vorticity ($10^{-5}\,s^{-1}$) and (b) potential vorticity fields ($10^{-6}\,m^2\,s^{-1}\,K\,kg^{-1}$) at 0000 UTC (0900 LST), March 19, 2001 at the beginning stage of the duststorm. Red circle on a red line from Neimongo–Seoul–Japan in (a) denotes negative relative vorticity area, which induces the generation of duststorm in (a). White, grey and dark color area in (b) indicate CBL of about 200 m thick with an ML of 1 km depth in Neimongo and stable layer of 200 m–700 m in the other area. Red circle denotes duststorm area in unstable CBL.
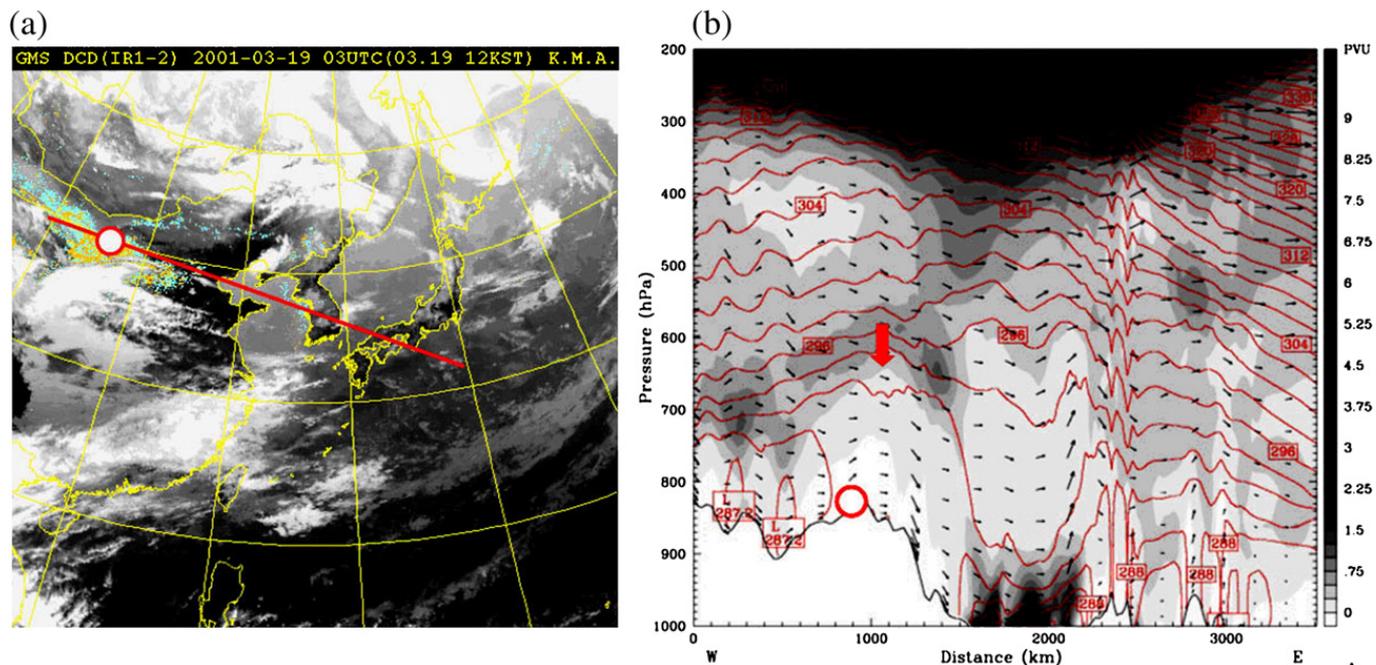
Fig. 13. (a) GMS (DCD-IRI-2) image at 0300 UTC (1200 LST) and (b) PV on March 19, 2001. Red line in (b) is potential temperature. The 0300 UTC image with partial cloud cover was used instead of poorly resolved 0000 UTC image. Duststorm area in the satellite image on the straight red line coincides with the CBL—white color at the mountain sites near red circle area in (b). Red arrow indicates the line (level) of $\partial\theta/\partial p = 0$, between dark and lighter grey layers and this level limits the rise of dust particles.

layer (i.e., CBL about 200 m thick) existed over the highest mountain surface in Neimongo, and a relatively larger ML over 1.5 km in depth up to the height of $\partial\theta/\partial p = 0$ existed above the CBL as it further developed over daytime hours (Fig. 13a,b).

Above 700 hPa (approximately 3 km) (Fig. 12b), stability extended through the stratosphere. Below 700 hPa, the CBL (negative PV value; PVU<0) had a depth of about 1 km. Initially, dust particles in the CBL rose reaching the ML of about 1.5 km above the CBL. This means that during the day dust parcels were lifted to about 700 hPa where the potential temperature gradient with pressure ($\partial\theta/\partial p$) was zero. The height of these dust parcels was confined to the 700-hPa level where stability extended from the stratosphere to the 700-hPa level.

With dust particulate remaining inside the ML, the westerly wind drove the particles downwind. The reason that the ML was much thicker than the CBL may have been due to daytime, thermally induced, vertical-mixing processes with less than 40% RH (Fig. 14b,c) and mechanical-mixing processes by strong winds over 12 m s^{-1} (Fig. 14a,d) below the 700-hPa level. Since the baroclinic PV equation contained both thermal and mechanical processes with respect to time, one can trace easily the evolution of PV through the vertical and horizontal movement of air parcels. In particular, the negative vorticity area at the 500-hPa level, inducing upward motion of air from the ground surface (duststorm generation area), closely matched the dust distribution area shown on the GMS satellite images (Figs. 12 and 13).

3.2. Origin of air masses during duststorms

In order to investigate the cause of dust transport from its generation areas in southern Mongolia and northwest China (Gansu province) to Beijing, China, back trajectories were calculated every 6 h during the duststorm period from March 19 (developing stage) to March 20, 2001 (Fig. 15). Three layers from the ground surface to 10 km, namely, 500–1500 m (approximate depth of the boundary layer), 3000–4500 m (middle troposphere), and 5000–6000 m (upper troposphere including the effect of the stratosphere), were considered.

Air trajectories in the developing stage of the duststorm in China at 0000 UTC and 1200 UTC, March 19, 2001, indicated that air parcels in the upper and middle troposphere (5 km and 3 km, respectively) passed through the southern part of Mongolia and partially through the middle part of Mongolia, while in the lower troposphere (atmospheric boundary layer), air parcels continually passed through southern Mongolia. Back trajectories did not directly reflect all directions of moving air parcels but only the general direction. Propagation of dust particles to the east by the back trajectories did not well reflect the traces of dust particles on the satellite imagery. This method was not an adequate qualitative method for determining dust transport over an area of interest. Thus, the real-time evaluation of negative vorticity areas having a low RH of less than 40% and strong winds over 10 m s^{-1} may be a good indicator to predict duststorm generation areas and dust transport routes.

4. Conclusion

An area of maximum negative vorticity, which induced strong upward motion coincided with the area of the duststorm generation in inner Mongolia where RH was less than 30% and wind speed was greater than 7–8 m s^{-1}. Dust transport always follows the negative vorticity area downwind. The source region for the duststorm (maximum negative vorticity area) was the same as the layer of unstable atmospheric air (negative PV value) near the ground surface in the vertical distribution of

(a)

(b)

(c)

(d)
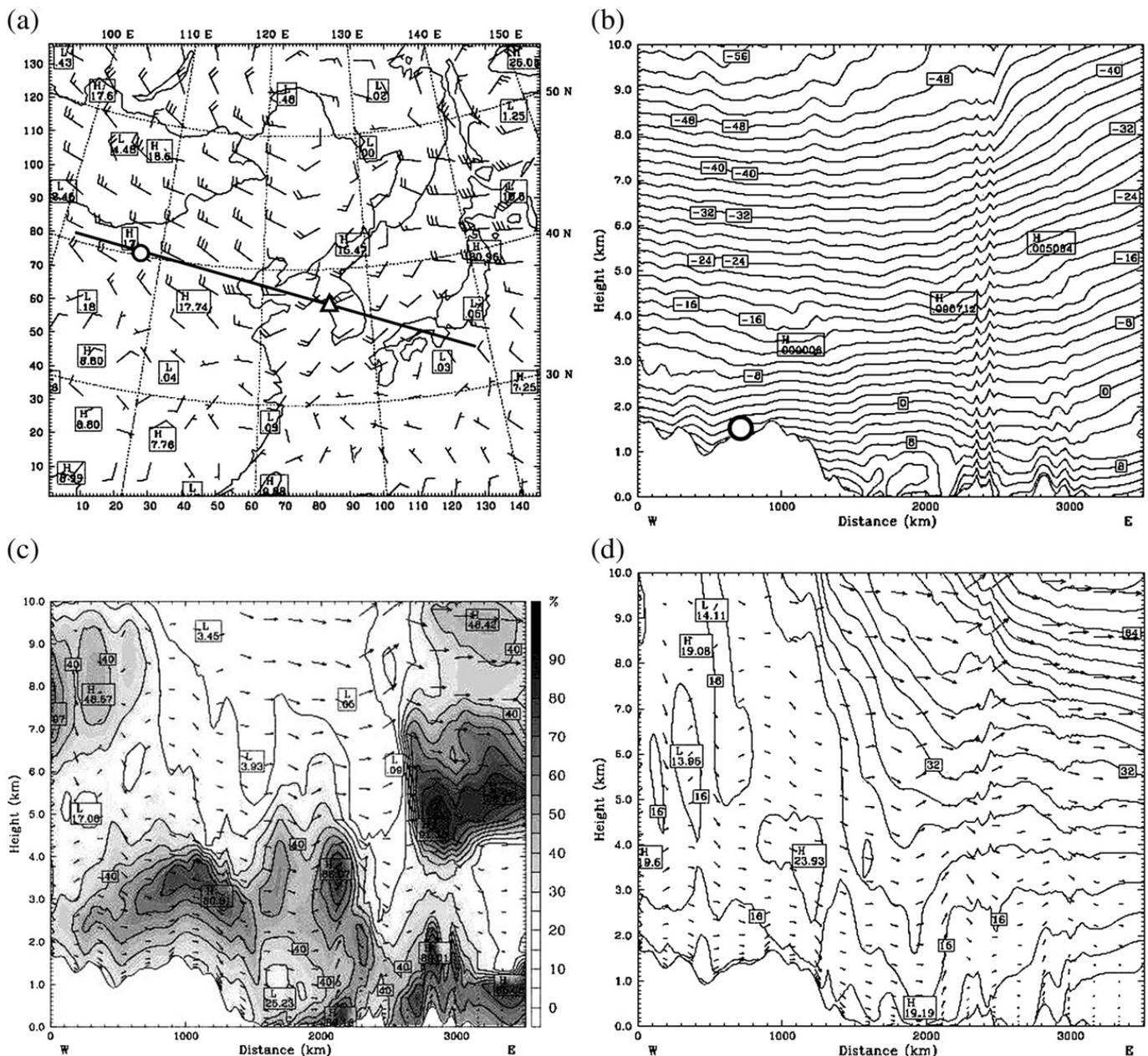
Fig. 14. (a) Horizontal wind vectors (m s^{-1}), (b) vertical distribution of air temperature (2 °C) with wind speed (m s^{-1}), (c) RH (%) with wind speed (m s^{-1}), and (d) horizontal wind speed (m s^{-1}) of 4 m s^{-1} of interval at 0300 LST, March 19, 2001. RH of 35%, air temperature of 6 °C, and wind speed greater than 12 m s^{-1} were detected in the circle area.

baroclinic PV, which is a function of diabatic heating and frictional terms with respect to time.

From PV during the day, air parcels (containing dust) rose to about 700 hPa (about 3 km) where the potential temperature gradient with pressure ($\partial\theta/\partial p$) was zero. Above 700 hPa, the troposphere was stable, and this stability was induced by stability from the stratosphere. Within the first 3 km, the CBL with a negative PV value existed with a depth of about 1 km, and initially, dust particles in the CBL rose from the ground surface reaching the ML, which was about 1.5 km thick above the CBL. While remaining inside the ML, dust particles were then driven downwind by the westerly wind. The depth of the CBL decreased early in the morning and late afternoon, but the ML changed little throughout the day. At

night, a shallow stable layer or nocturnal surface inversion layer with a large positive PV value developed due to nocturnal cooling of the ground, and particles inside the stable layer merged near the ground and moved downwind. Dust particles in the ML continued to move downwind, and dry deposition may have occurred as they descended from the top of the stable layer toward the ground surface.

Acknowledgements
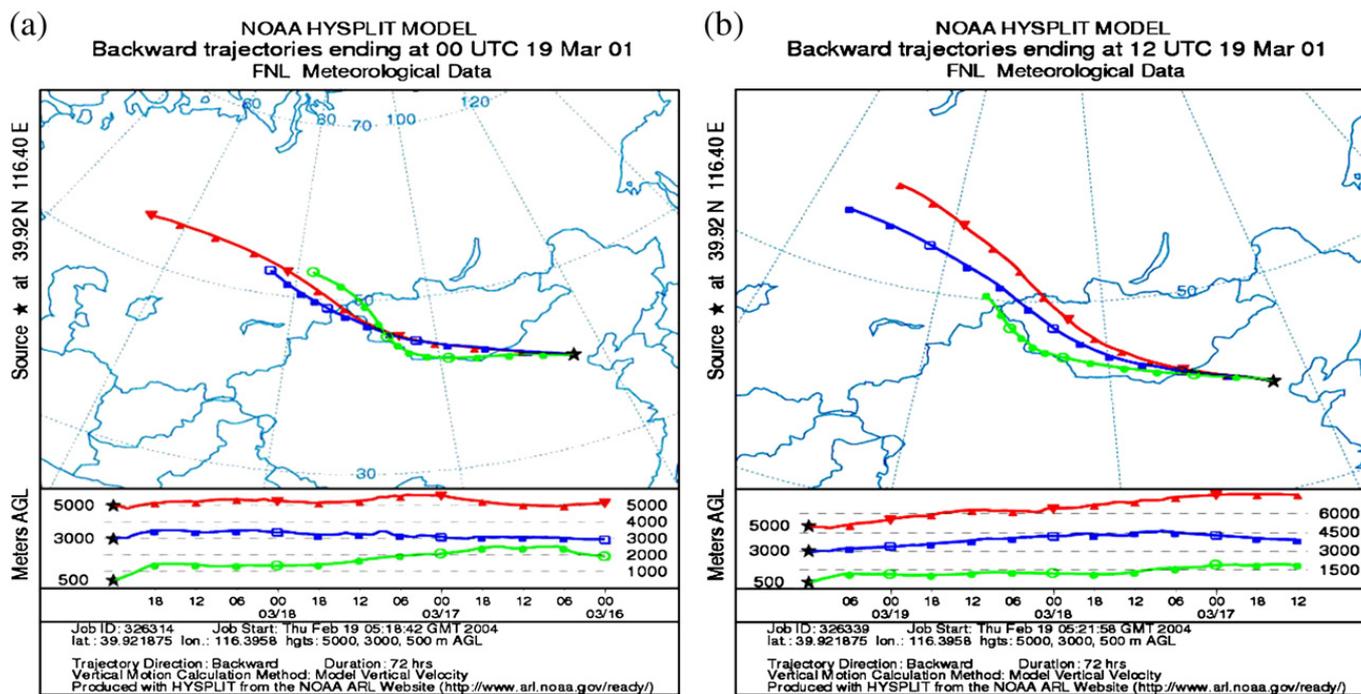
Fig. 15. Back trajectory at 6-hour intervals on 3 levels—5000 m (upper troposphere; red); 3000 m (middle troposphere; blue); and 500 m (lower troposphere; green) over Beijing at (a) 0000 UTC and (b) 1200 UTC, March 19, 2001.

References

Austin, J., Midgley, R., 1994. The climatology of the Jet Stream and stratospheric intrusions of ozone over Japan. Atmos. Environ. 28, 39–52.

Bluestein, H.B., 1993. Synoptic–Dynamic Meteorology in Midlatitudes, vol. 2. Oxford Univ. Press, pp. 180–219.

Carmichael, G.R., Hong, M.S., Ueda, et al., 1997. Aerosol composition at Cheju Island. Korea. J. Geophys. Res. 102 (5), 6047–6061.

Chen, S.J., Kuo, Y.H., Zhang, et al., 1991. Synoptic climatology of cyclogenesis over east Asia, 1958–1987. Mon. Weather Rev. 119, 1407–1418.

Choi, H., Zhang, Y.H., Takahashi, S., 2004. Recycling of suspended particulates by the interaction of sea–land breeze circulation and complex coastal terrain. Meteorol. Atmos. Phys. 87, 109–120.

Chon, H., 1994. Historical records of yellow sand observations in China. Res. Environ. Sci. 7–6, 1–11.

Chung, Y.S., Yoon, M.B., 1996. On the occurrence of yellow sand and atmospheric loadings. Atmos. Environ. 30, 2387–2397.

Chung, Y.S., Kim, H.S., Jugder, D., et al., 2003. On sand and duststorms and associated significant dustfall observed in Chongju-Chongwon, Korea. Water Air Soil Pollut.: Focuss 3, 5–19.

Haynes, P.H., McIntrye, M.E., 1987. On the evolution of vorticity and potential vorticity in the presence of diabatic heating and frictional or other forces. J. Atmos. Sci. 44, 828–841.

Holton, J.R., 1992. An Introduction to Dynamic Meteorology, 3rd Ed. Academic Press, pp. 87–145.

Hong, S.Y., Pan, H.L., 1996. Nonlocal boundary layer vertical diffusion in a medium-range forecast model. Mon. Weather Rev. 124, 2322–2339.

Jigjidsuren, S., Oyuntsetseg, S., 1998. Pastureland Utilization Problems and Ecosystem, vol. 2. Ecological Sustainable Development, Ulaanbaatar, pp. 206–212.

Jungder, D., 1999: Hydrodynamic statistic model for prediction of wind, snow storms and dust storms over the territory of Mongolia. The thesis presented for Ph.D. in mathematics and physics. National University of Mongolia, Ulaanbaatar, 3–30.

Middleton, N.J., 1986. A geography of dust storms in southwest Asia. J. Climate 6, 183–196.

Natsagdorj, L., Jugder, D., 1992a. Statistics Method for Prediction of Dust Storms over the Gobi and Steppe Area in Mongolia in Spring. Scientific report, Ulaanbaaatar, p. 83.

Natsagdorj, L., Jugder, D., 1992b. Dust storms in the Mongolian Gobi. Proc. of the Symposium on Global Change and the Gobi Desert, Ulaanbaatar, pp. 25–40.

Qian, Z., Hu, Y., 1997. Survey and Analysis for "93.5.5." Strong Dust Storm, Dust Storm Research in China. Meteorology press, Beijing, pp. 37–43.

Reed, R.J., 1979. Cyclogenesis in polar air stream. Mon. Weather Rev. 107, 38–52.

Reed, R.J., Sanders, F., 1953. An investigation of the development of a mid-tropospheric frontal zone and its associated vorticity field. J. Meteorol. 10, 338–349.

Reed, R.J., Albright, M.D., 1986. A case study of explosive cyclogensis in the Eastern Pacific. Mon. Weather Rev. 114, 2297–2319.

Rossby, C.G., (collab), 1937. Isentropic analysis. Bull. Am. Meteorol. Soc. 18, 201–209.

Rossby, C.G., 1940. Planetary flow patterns in the atmosphere. Q. J. R. Meteorol. Soc. 66, 68–87 Suppl.

Sanders, F., Gyakum, J.R., 1980. Synoptic–dynamic climatology of the "bomb". Mon. Weather Rev. 108, 1589–1606.

Tegen, I., Fung, I., 1994. Modeling of mineral dust in the atmosphere: source transport and potical thickness. J. Geophys. Res. 99 (D11) 22987–22914.

Wang, X., Ma, Y., Chen, H., Wen, G., Chen, S., Tao, Z., Chung, Y., 2003. The relation between sandstorms and strong winds in Xinjiang, China. Water Air Soil Pollut.: Focus 3, 67–79.

Xuan, J., Sokolik, I.N., 2002. Characterization of sources and emission rates of mineral dust in Northern China. Atmos. Environ. 36, 4863–4876.

Yamamoto, K., Aoyama, M., Ito, K., Kasahara, M., Kitada, T., Kurata, G., 2003. Development of long range transport model for mineral dust in east Asia. Proc. of ASSQ conference, March, Tsukuba, Japan.

Zhang, Y., Zhong, Y., 1985. The simulation and diagnosis for a strong wind associated with northeast low. Acta Meteorol. Sin. 43, 97–105.